processes

MDPI

Article

Study on the Medium-Temperature Reduction Behavior of Methane and Laterite Nickel Ore

Ying Shi [1,2], Sheng Qi [1,2], Xingyang Liu [1,2], Shoujun Liu [1,2], Jinyao Yan [3] and Song Yang [1,2,*]

[1] College of Chemistry and Chemical Engineering, Taiyuan University of Technology, Taiyuan 030024, China; shiying0307@163.com (Y.S.); qiisheng@163.com (S.Q.); yliu22918@gmail.com (X.L.); 13303460889@163.com (S.L.)
[2] Shanxi Engineering Center of Civil Clean Fuel, Taiyuan University of Technology, Taiyuan 030024, China
[3] Taiyuan No. 5 Middle School, Taiyuan 030012, China; yjy20060908@163.com
* Correspondence: yangsong@tyut.edu.cn; Tel.: +86-132-3362-0827

Abstract: Under the background of carbon peaking and carbon neutrality, compared with a traditional carbon thermal reduction to produce nickel, gas-based reduction has outstanding advantages in efficiency and carbon reduction. However, there are few studies on gas-based reduction at present. This article explores the reduction behavior of methane on laterite nickel ore. The effects of different reaction temperatures, reaction times and gas concentrations on the reduction reaction were studied. The phase and morphology of laterite nickel ore and its calcined products were analyzed by XRD, SEM-EDS and gas chromatography. The results show that when the reduction temperature is 900 °C, the reduction time is 60 min, and the concentration of CH_4 is 50%, a concentrate with a nickel grade of 3.06% and a recovery of 52.09% can be obtained. After analysis, the reason for the low nickel grade and recovery rate in the concentrate is, on the one hand, due to the incomplete reduction of NiO, and a large amount of nickel still exists in the silicate in the tailings; on the other hand, it is due to the fine grain size of the partially reduced nickel iron alloy, which is lost in the tailings and filtrate.

Keywords: laterite nickel ore; methane; reduction behavior; nickel-iron alloy; nickel-iron migration

Citation: Shi, Y.; Qi, S.; Liu, X.; Liu, S.; Yan, J.; Yang, S. Study on the Medium-Temperature Reduction Behavior of Methane and Laterite Nickel Ore. *Processes* **2023**, *11*, 3291. https://doi.org/10.3390/pr11123291

Academic Editors: Weiwei Xuan and Markus Reinmöller

Received: 11 October 2023
Revised: 20 November 2023
Accepted: 23 November 2023
Published: 24 November 2023

1. Introduction

Nickel is an important metal for the development of modern technology. Nickel mainly comes from nickel sulfide ore and laterite nickel ore [1]. In the past, industrial production of nickel mainly relied on nickel sulfide [2]. However, due to the widening gap between the supply and demand of nickel resources, laterite nickel ore has also become an important source of nickel production [3]. But its complex mineral composition leads to a low nickel recovery rate. Therefore, developing and optimizing the process of extracting nickel from laterite nickel ore is of great significance for the industrial production of nickel [4].

Among the commonly used nickel production methods, pyrometallurgy is suitable for large-scale production [5], but it can lead to a large amount of energy waste. Hydrometallurgical processes are more energy efficient [6], but the process is complex and has stricter requirements for minerals [7–9].

Researchers have been exploring methods to improve the magnetic separation process of laterite nickel ore roasting, one of which is to use different reducing agents. The commonly used types of reducing agents include solid-based reducing agents (anthracite or coke) and gas-based reducing agents (CO, H_2, CH_4, etc.). Su et al. (2022) used carbon as a reducing agent in their experiment and increased the grade of nickel in the concentrate with the help of additives [10]. However, the high temperature of carbon thermal reduction and the large amount of carbon dioxide emissions do not meet the current policy requirements of carbon peaking and carbon neutrality. Man et al. [11] used 2% bituminous coal as a reducing agent, and obtained a nickel grade of 10.86% and a nickel recovery rate of 88.56% at a roasting temperature of 1200 °C, a sodium sulfate addition of 10%, and a roasting

time of 50 min. However, the reaction temperature of carbon thermal reduction is too high, the energy consumption is too high, and the reduction degree of the solid–solid phase reaction is difficult to control. Direct reduction of laterite nickel ore by gas-based reducing agents belongs to a gas–solid phase reaction, which has many advantages such as a low reduction temperature and sufficient reaction. Hu et al. [12] studied the kinetics of reduction roasting reaction of laterite nickel ore in CO atmosphere. Under the conditions of a roasting temperature of 900 °C and a roasting time of 3 h, a nickel reduction rate of 79.47% and a metallization rate of 60.27% were obtained. The purpose of studying the reducibility of CO is mostly to deepen the understanding of the reduction degree during the carbon thermal reduction process, and almost no consideration is given to use CO as the single reducing agent to directly reduce laterite nickel ore. H_2 as a reducing agent can significantly reduce the reduction temperature of laterite nickel ore and greatly increase the reduction reaction rate. Lu et al. [13] obtained a nickel grade of 6.38% and a nickel recovery rate of 91.07% under conditions of a H_2 atmosphere, an Na_2SO_4 additive ratio of 20 wt.%, a roasting temperature of 800 °C, and a roasting time of 220 min. However, due to the low utilization rate and high price of H_2, its application is limited to some extent. As a reducing agent for reducing laterite nickel ore, CH_4 not only has a wide source of methane compared to other reducing agents, but also has a low operating temperature, reducing the cost of smelting. Therefore, many scholars have conducted research on methane reduction of laterite nickel ore. Mohanty et al. [14] studied the reduction reaction of laterite nickel ore using CH_4 as a reducing agent and found that CH_4 has good reduction performance in the temperature range of 400–800 °C. They believe that CH_4 can be used as a reducing agent for direct reduction of laterite nickel ore.

In the reduction stage of the roasting magnetic separation process of laterite nickel ore, iron oxide can be reduced to FeO by controlling the reduction conditions, while nickel can be recovered. FeO is non-magnetic and does not exist in the concentrate during the magnetic separation stage. Therefore, controlling the reduction of iron oxide is crucial for improving the nickel grade of the final product [15].

Based on previous research results, this article studied the reaction behavior of reducing laterite nickel ore using methane as a reducing gas and roasting magnetic separation method from both theoretical and experimental perspectives. The recovery rate and grade of nickel under different reduction reaction conditions were analyzed, and the migration behavior of nickel was studied through scanning electron microscopy energy dispersive spectroscopy (SEM-EDS) and X-ray diffraction (XRD). The reasons for the low nickel grade and recovery rate were analyzed. The research results provide new ideas and methods for the development of gas-based reduction.

2. Experimental

2.1. Experimental Materials

The laterite nickel ore used in this experiment came from Sulawesi, Indonesia, and it was a transition laterite nickel ore. The chemical composition of the initial ore is shown in Table 1.

Table 1. The main chemical composition of nickel laterite ore (wt.%).

Fe	Ni	Al	Ca	Mg	Cr	Si	O	Mn	Co
25.37	1.65	2.57	0.12	7.06	0.89	6.71	47.10	0.62	0.07

The XRD curve of the laterite nickel ore is shown in Figure 1. The main crystalline phases of the raw ore were serpentine ($Mg_3Si_2O_5(OH)_4$), goethite (FeOOH), hematite (Fe_2O_3), iron serpentine ($Fe_4SiO_4(OH)_5$), and quartz (SiO_2). Due to the low grade of nickel in the raw ore, the phase of nickel cannot be detected.

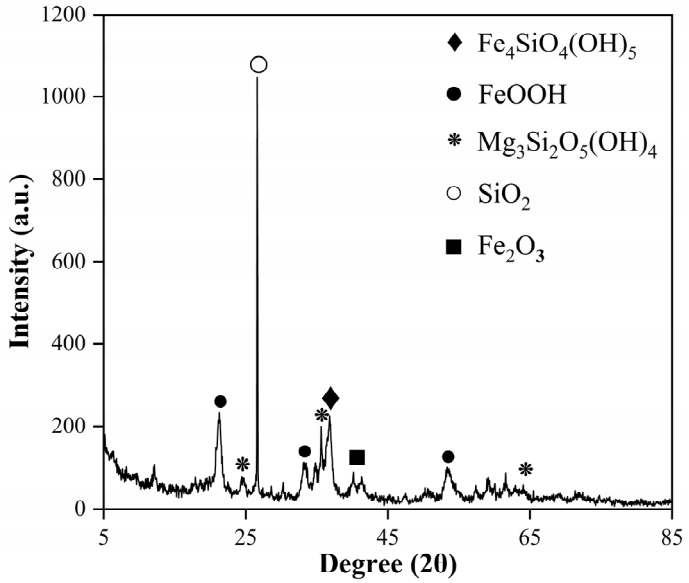

Figure 1. XRD curve of laterite nickel ore.

The diffraction peaks at 18.9°, 35.6°, and 53.2° corresponds to the (002), (110), and (114) crystal planes of FeOOH (PDF # 46-1315), respectively. The diffraction peaks at 25.5°, 34.6°, and 65.7° corresponds to the (111), (200), and (005) crystal planes of $Mg_3Si_2O_5(OH)_4$ (PDF # 22-1164), respectively. The diffraction peak at 26.2° corresponds to the (101) crystal plane of SiO_2 (PDF # 11-0252), and the diffraction peak at 41.5° corresponds to the (521) crystal plane of Fe_2O_3 (PDF # 16-0653).

2.2. Experimental Methods

The schematic diagram of the experimental equipment used in this experiment is shown in Figure 2, and the experimental process is shown in Figure 3 [16]. Firstly, 50 g of laterite nickel ore is weighed and loaded into the reactor. The water cooling device is turned on, and the protective gas N_2 is introduced (with a gas flow rate of 100 mL·min^{-1}). Then, a heating program is set to raise the temperature to the set temperature (with a temperature range of 600 °C~1200 °C). When the temperature reaches the required temperature for the experiment, a quantitative amount of CH_4 gas is introduced for reduction (with a CH_4 gas flow rate of 150 mL·min^{-1}), and the reduction time is 60–90 min. After the reduction phase is completed, turn off the heating device, stop introducing methane, and cool to room temperature under N_2 protection. After cooling to room temperature, the roasted ore is taken out, and after sample preparation in the prototype, 5 g of the sample is taken out for magnetic separation in a wet weak magnetic separator with a current intensity of 2 A.

The grade of the concentrate after magnetic separation is calculated using the dimethylglyoxime photometric method, and the nickel recovery rate is calculated using Equation (1):

$$\varepsilon = \left(\frac{m_1 \times \alpha_1}{m_0 \times \alpha_0}\right) \times 100\% \quad (1)$$

In the equation: ε is the nickel recovery rate, %; α_1 is the nickel grade in the concentrate, %; α_0 is the nickel grade in the raw ore, %; m_1 is the mass of magnetic separation concentrate, g; m_0 is the mass of the magnetic separation raw ore, g.

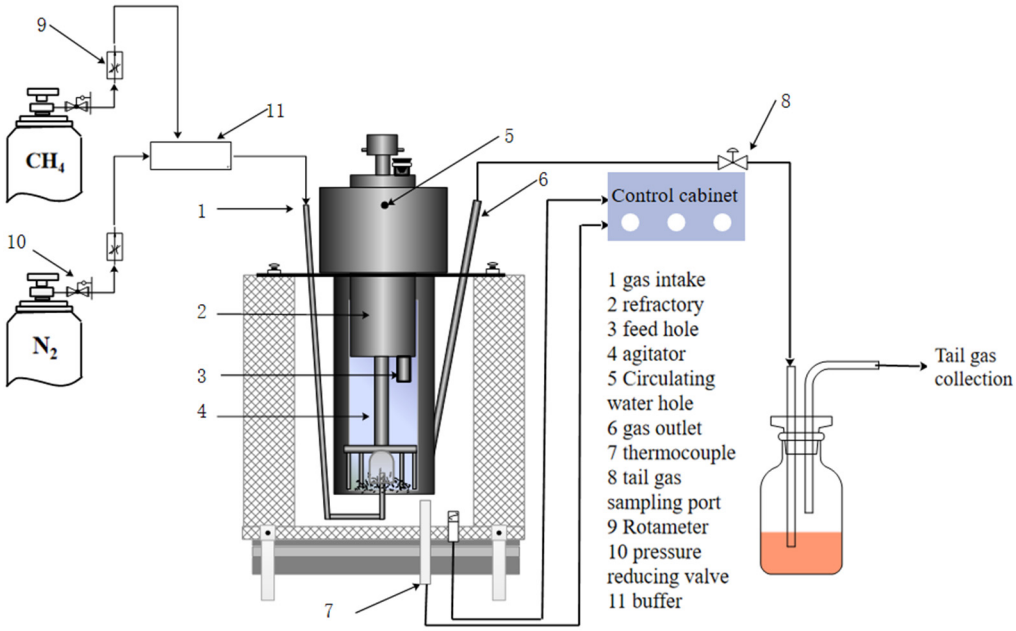

Figure 2. Experimental procedure schematic diagram of reduction of nickel laterite.

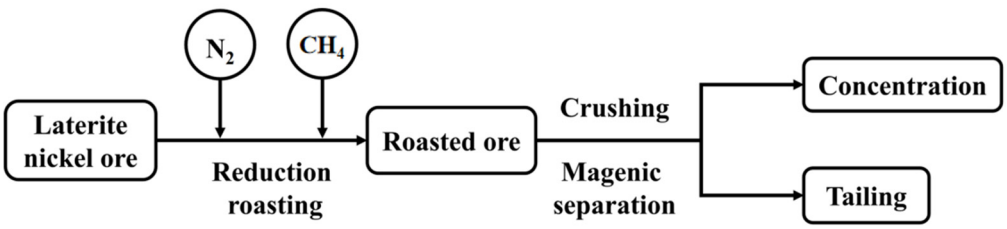

Figure 3. Experimental flowchart of methane reduction of laterite nickel ore.

2.3. Characterization and Analysis

This experiment used the D/MAX2500 X-ray diffractometer produced by Rigaku Company in Japan to conduct X-ray diffraction analysis on the raw ore, reduction roasting products, concentrate, and tailings, and to investigate the crystal structure and change patterns. Working conditions: Cu-Kα as a radiation source, a graphite monochromatic tube (U = 40 kV, I = 100 mA) is used, with a scanning rate of $4^\circ \cdot min^{-1}$ and a scanning range of 5°~85°.

The morphology, element types, and distribution content of the samples were analyzed using the EVOHD15 scanning electron microscope produced by Zesis company (Shanghai, China) combined with electron spectroscopy (SEM-EDS).

Analyze the exhaust gas generated during the roasting process using the GC-7820 chromatograph from Beijing Zhongke Huifen Instrument Co., Ltd. (Beijing, China).

3. Results and Discussion

3.1. Thermodynamic Study on the Reduction Reaction between Methane and Laterite Nickel Ore

The Gibbs free energy is the basis for determining whether a reaction can proceed spontaneously. If $\Delta G^\theta \leq 0$, the reaction is spontaneous. The corresponding formula is as follows:

$$\Delta G_T^\theta = \Delta H_{298}^\theta - T\Delta S \quad (2)$$

In the formula [16], G is the Gibbs free energy, in units of J, H is the total thermodynamic energy of the system in units of J, T is the temperature, in units of °C, and S is the entropy of the system in units of J/°C. All data involved in the calculation are obtained from the thermodynamic data manual.

The cracking reaction equation of methane is as follows:

$$CH_4(g) \rightarrow C + 2H_2(g)\Delta G = -0.0125T + 83.032 \quad (3)$$

The possible reactions that may occur when methane alone reduces laterite nickel ore are as follows:

$$4NiO + CH_4(g) \rightarrow 4Ni + CO_2(g) + 2H_2O(g)\Delta G = -0.3544T + 148.76 \quad (4)$$

$$12Fe_2O_3 + CH_4(g) \rightarrow 8Fe_3O_4 + CO_2(g) + 2H_2O(g)\Delta G = -0.5775T + 171.44 \quad (5)$$

$$4Fe_3O_4 + CH_4(g) \rightarrow 12FeO + CO_2(g) + 2H_2O(g)\Delta G = -0.4505T + 422.77 \quad (6)$$

$$4FeO + CH_4(g) \rightarrow 4Fe + CO_2(g) + 2H_2O(g)\Delta G = -0.2637T + 259.1 \quad (7)$$

By consulting thermodynamic data and using regression analysis, plot the Gibbs free energy diagram of ΔG~T shown in Figure 4. According to Equation (4), when the temperature is greater than 146.85 °C, the reaction of methane reducing NiO will occur. When the temperature is greater than 23.85 °C, 664.85 °C, and 709.85 °C, the reaction of methane reducing iron oxide will proceed in the following order: $Fe_2O_3 \rightarrow Fe_3O_4 \rightarrow FeO \rightarrow Fe$. Moreover, the reaction temperature required for the reduction of iron oxides to FeO and Fe is relatively high, both exceeding 626.85 °C. Therefore, by controlling the reaction temperature reasonably, the reduction of iron oxides can remain in the FeO stage, and non-magnetic iron oxides can be removed during the magnetic separation stage.

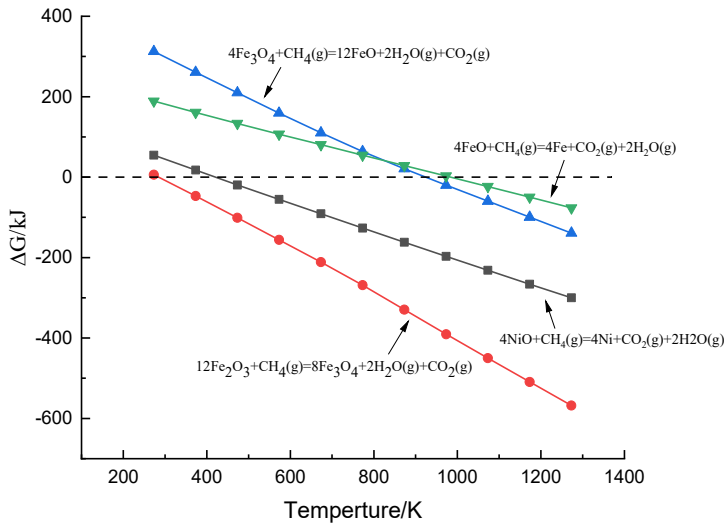

Figure 4. Thermodynamic Equilibrium Diagram of CH_4 Reduction of Iron and Nickel Oxides.

The possible reactions between nickel oxide and iron oxide under H_2 atmosphere are as follows:

$$NiO + H_2(g) \rightarrow Ni + H_2O(g)\Delta G = 0.0363T - 7.5911 \quad (8)$$

$$3Fe_2O_3 + H_2(g) \rightarrow 2Fe_3O_4 + H_2(g)\Delta G = -0.0921T - 1.9213 \quad (9)$$

$$Fe_3O_4 + H_2(g) \rightarrow 3FeO + H_2O(g)\Delta G = -4.3986T + 42.343 \quad (10)$$

$$FeO + H_2(g) \rightarrow Fe + H_2O(g)\Delta G = -0.0136T + 19.995 \quad (11)$$

By consulting thermodynamic data and using regression analysis, plot the Gibbs free energy diagram of ΔG~T shown in Figure 5. According to Equations (8) and (9), it can be calculated that ΔG is less than 0 in the temperature range of 25–1200 °C, indicating that these two reactions are very unstable in the presence of H_2 and are easily reduced by H_2 to Ni and Fe_3O_4. The reduction of iron oxides is carried out in three stages, $Fe_2O_3 \rightarrow Fe_3O_4 \rightarrow FeO \rightarrow Fe$. As the temperature increases, the reaction proceeds step by step. According to Equation (10), when the temperature is greater than 419.85 °C, the Gibbs free energy of the reaction is less than zero, indicating that the process of Fe_3O_4 reduction to FeO is greatly affected by temperature. The higher the temperature, the more FeO is generated. Equation (11) represents the reaction of FeO reduction to Fe, and the Gibbs free energy of this reaction is greater than zero within the temperature range studied in the experiment. This indicates that this reaction is almost impossible to occur spontaneously, and the Fe can only be generated at extremely high temperatures.

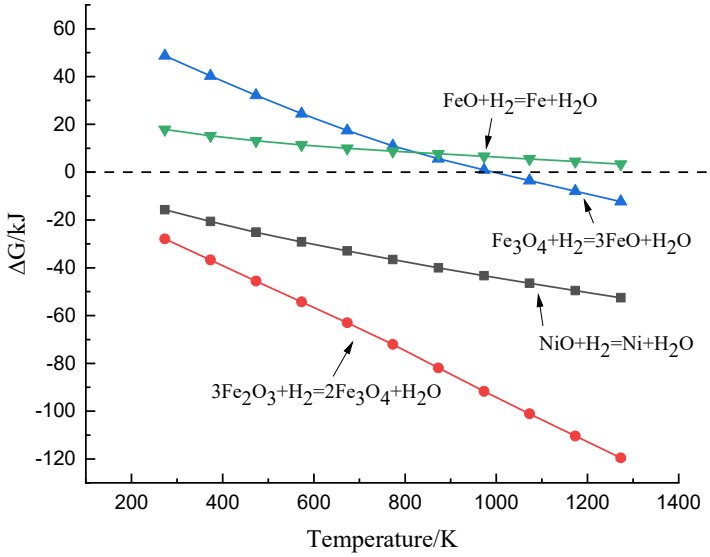

Figure 5. Thermodynamic equilibrium diagram of H_2 reduction of iron and nickel oxides.

3.2. Reduction Reaction Conditions of Methane with Laterite Nickel Ore

3.2.1. The Effect of Reduction Reaction Temperature on the Grade and Recovery Rate of Nickel Iron

At the reduction reaction temperatures of 600 °C, 700 °C, 800 °C, and 900 °C, with a reduction reaction time of 60 min and a CH_4 concentration of 100%.The results shown in Figure 6 indicate that the nickel grade and recovery rate increase as the temperature increases from 600 °C to 800 °C. At a reduction temperature of 800 °C, the peak nickel grade is 2.6%, and the corresponding recovery rate is 55.24%. It is worth noting that in laterite nickel ore, some nickel iron oxides form a serpentine phase, which makes it difficult to reduce this nickel at low temperatures [17]. At 900 °C, although the reduction process of iron oxide continued, the recovery rate of nickel did not increase. During the magnetic separation stage, a significant amount of iron was recovered, reducing the nickel grade.

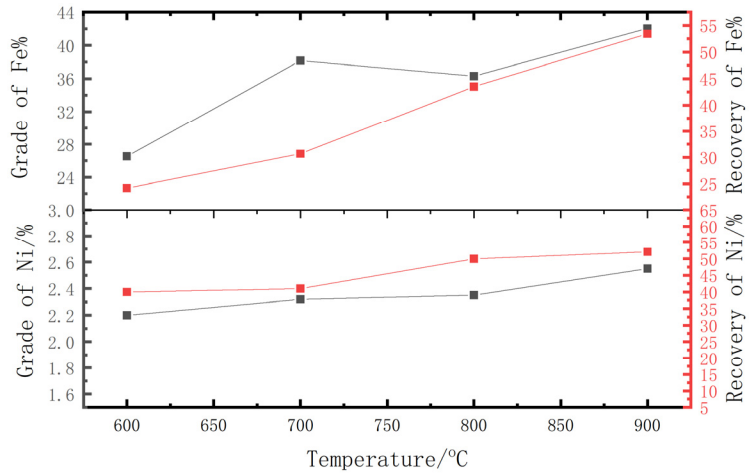

Figure 6. The Effect of Reduction Reaction Temperature on the Grade and Recovery Rate of Nickel and Iron.

3.2.2. The Effect of Reduction Reaction Time on the Grade and Recovery Rate of Nickel Iron

At a reduction reaction temperature of 900 °C, a CH_4 concentration of 100%, and a reduction reaction time of 30 min, 60 min, 90 min, and 120 min, respectively. The results are shown in Figure 7. Due to the inability of the stable nickel lattice in silicate ore to react with CH_4, most nickel oxides are reduced after 30 min. After 60 min, the nickel grade and recovery reached peaks of 2.66% and 52.19%, respectively. However, when the reduction reaction time increases from 60 min to 90 min, methane cracking leads to solid carbon deposition, hindering gas diffusion [18,19]. In addition, the oxygen in the ore oxidizes some nickel metals, reducing the nickel recovery rate. When the reduction time exceeds 90 min, the reducing gas diffuses into the particles, reducing the oxides of nickel and iron and improving the nickel recovery rate. As time goes by, the recovery rate of iron gradually increases, and the iron content in the magnetic separation concentrate continues to increase. The longer reaction time leads to a decrease in nickel content in the concentrate.

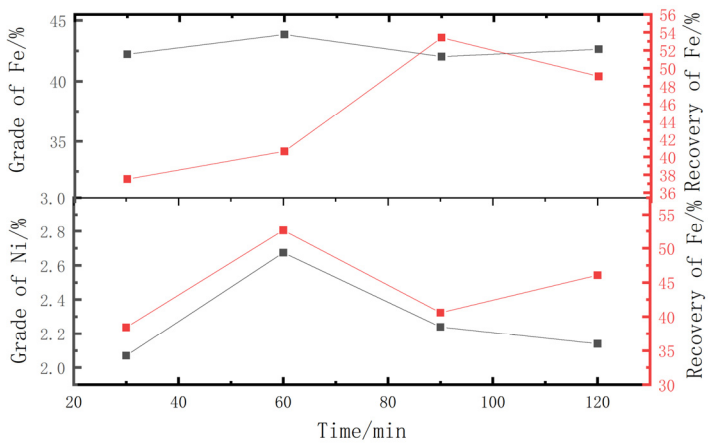

Figure 7. The Effect of Reduction Reaction Time on the Grade and Recovery Rate of Nickel and Iron.

3.2.3. The Effect of Methane Concentration on the Grade and Recovery Rate of Nickel Iron

As shown in Figure 8, experiments were conducted at a reduction reaction temperature of 900 °C, a reduction reaction time of 60 min, and CH_4 concentrations of 15%, 25%, 35%, 50%, and 100%, respectively. Initially, the improvement of CH_4 diffusion enhanced the reducing atmosphere, thus increasing the concentration of CH_4 and increasing the grade and recovery rate of nickel. However, with the progress of the experiment, methane

cracking generates carbon black. The accumulation of carbon black hinders the gas–solid reaction, reducing the grade and recovery rate of nickel iron. When the CH_4 concentration is 50%, nickel oxide is completely reduced. When the CH_4 concentration is 100%, the reduction reaction of iron oxide is enhanced, but the nickel recovery rate does not increase. During the magnetic separation stage, a significant amount of iron was recovered, resulting in a decrease in nickel content.

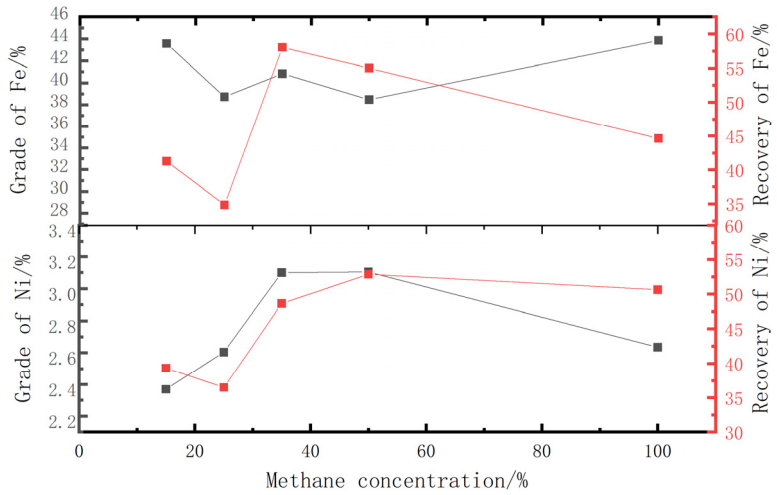

Figure 8. The Effect of Methane Concentration on the Grade and Recovery Rate of Nickel and Iron.

Through experiments, the optimal experimental conditions were determined as a reduction temperature of 900 °C, a reduction time of 60 min, and a CH_4 concentration of 50%. Under these conditions, the grade and recovery rate of nickel were 3.06% and 52.09%, respectively.

3.3. Migration of Nickel and Iron in Laterite Nickel Ore during Methane Reduction Process

By changing the reduction reaction conditions, the nickel recovery rate and content in the concentrate can be changed. However, the loss of nickel is inevitable. On the condition of a reduction time of 60 min, and a CH_4 concentration of 50%, this section measures the recovery rate and content of nickel in the concentrate, tailings, and tailings filtrate during the roasting and magnetic separation processes at different temperatures and describes the migration of nickel and iron. The results are shown in Figures 9 and 10.

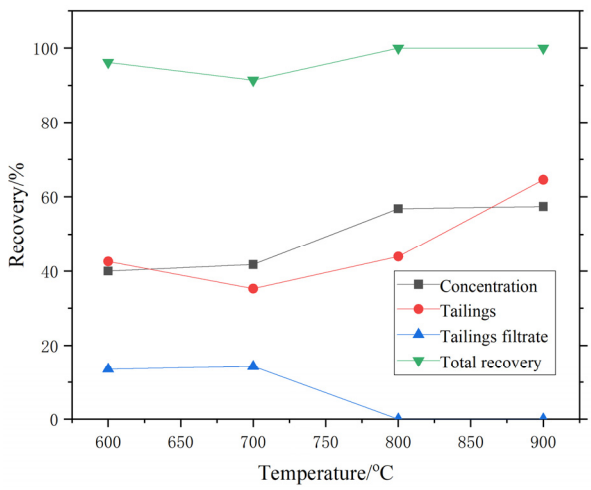

Figure 9. Recovery rate of nickel in concentrate, tailings, and tailings filtrate at different temperatures.

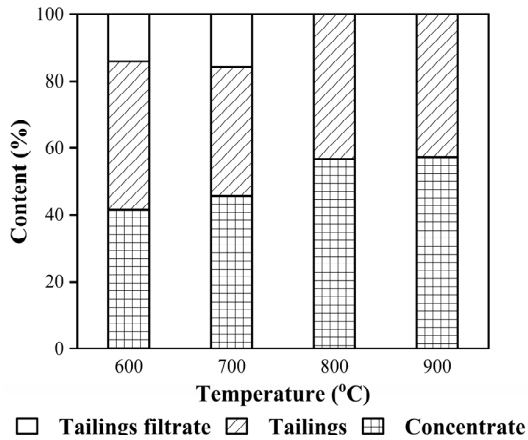

Figure 10. Content of nickel in concentrate, tailings, and tailings filtrate at different temperatures.

From Figures 9 and 10, it can be seen that nickel after magnetic separation mainly occurs in concentrate and tailings, and their recovery rates are almost equal, which is consistent with the research results of Pickles and Anthony (2018) [20]. When the temperature is low, a portion of nickel will also be lost in the filtrate of the tailings, with a recovery rate of 14–16% for this portion of nickel.

3.3.1. XRD Phase Analysis

In the XRD curve corresponding to Figure 10, the diffraction peak at 43.3° corresponds to the (200) crystal planes of NiO (PDF#47-1049). The diffraction peaks at 45.5°, 63.7°, 84.1° corresponds to the (002), (102), (103) crystal planes of {Fe,Ni} (PDF#26-0790). The diffraction peaks at 31°, 34.7°, 48.6° corresponds to the (040), (220), (143) crystal planes of $\{Mg,Fe\}_2SiO_4$ (PDF#37-0415).

The roasting temperature of laterite nickel ore affects the nickel content of the roasted ore and tailings. As shown in Figure 11, when the ore is reduced at 100% CH_4 concentration for 90 min, the morphology of nickel changes as the temperature increases from 600 to 900 °C. At 600 °C, nickel mainly exists in the form of nickel oxide in the roasted ore. However, when the temperature rises above 700 °C, due to the reaction of H_2 and CH_4 with nickel iron oxide, the nickel oxide phase disappears and {Fe, Ni} alloy phases appear. In addition, minerals like lizardstone and olivine hinder iron reduction [21,22]. Tailings are mainly composed of magnesia, silica, and carbon black, indicating that the recovery of iron oxide in minerals is incomplete. Carbon black blocks the pores on the mineral surface, hinders the diffusion of reducing gases, leading to an incomplete reduction of iron oxide [23]. In addition, there are also some nickel and iron in the form of silicates in the tailings, which reduces the recovery rate of the tailings.

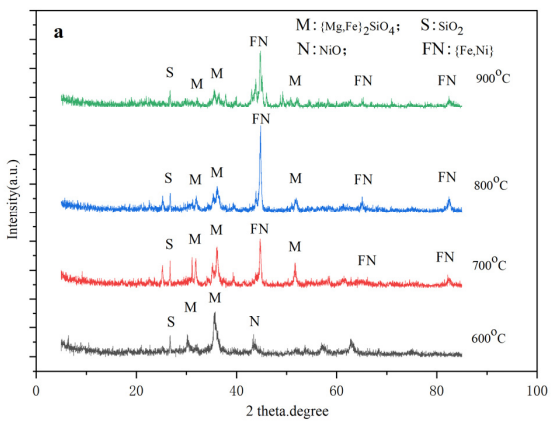

Figure 11. *Cont.*

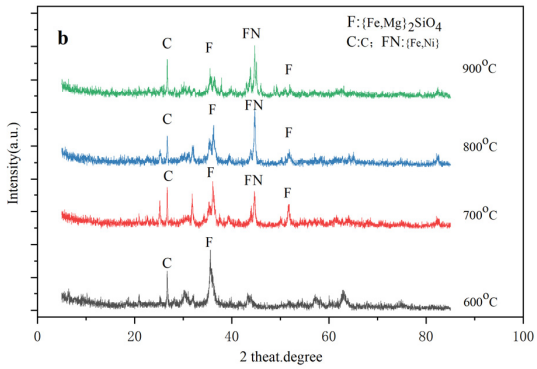

Figure 11. XRD curve of roasted ore (**a**) and tailings (**b**) at different temperatures.

3.3.2. SEM-EDS Analysis

Due to the low content, complex phase, and extremely fine particle size of nickel in laterite nickel ore, some Ni replaces some Mg^{2+} and Fe^{2+} in isomorphic form and integrates into the lattice of serpentine and goethite, making it difficult to control the degree of reduction. Through direct reduction with reducing agents, ideal nickel and iron grades and recovery rates cannot be obtained [24].

SEM-EDS analysis (Figure 12) shows that nickel and iron are relatively evenly distributed in the concentrate and tailings. However, thermodynamic analysis shows that CH_4 is difficult to reduce nickel in silicate minerals, and nickel in tailings exists in the form of nickel silicate. XRD analysis confirmed this, and no nickel oxide phase was found in the tailings. The size of iron nickel alloy particles was determined using backscatter spectroscopy and energy dispersive spectroscopy (Figure 13). The rich iron nickel area appears as a bright white area, and there is no obvious bright white area in the entire tailings. This indicates that the content of iron and nickel in tailings is lower than that in concentrates. In addition, the maximum particle size of iron nickel concentrate is approximately 3 μm. The minimum particle size is approximately 1 μm. In contrast, the particle size of tailings is smaller than that of concentrate, less than 1 μm. Due to the inability of this magnetic separation process to recover nickel and iron with such small particle sizes, some nickel is lost in the tailings. The energy spectrum analysis of tailings shows that the content of magnesium and silicon in tailings is high, indicating that the silicate in tailings is well preserved. It is challenging to recover nickel from tailings under experimental conditions.

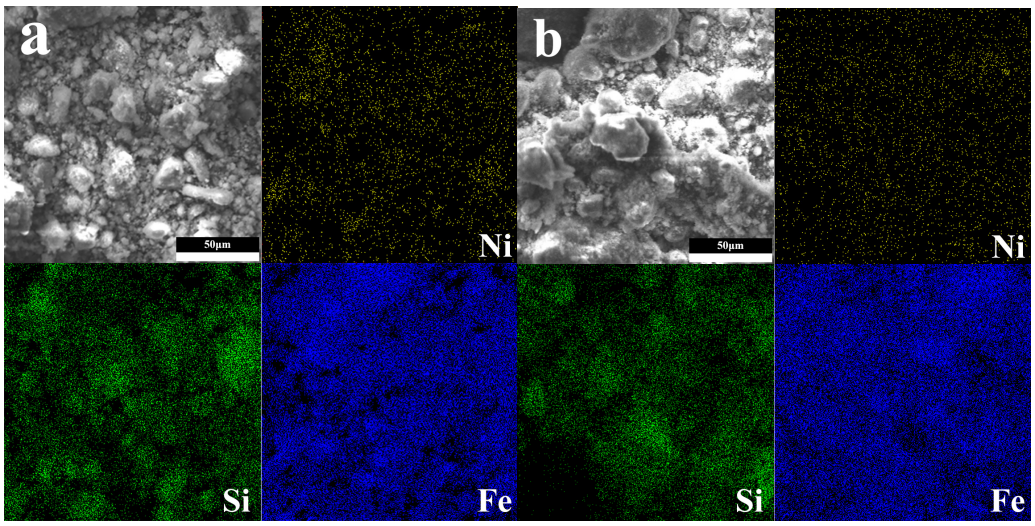

Figure 12. SEM-EDS spectra of concentrate (**a**) and tailings (**b**) at 900 °C.

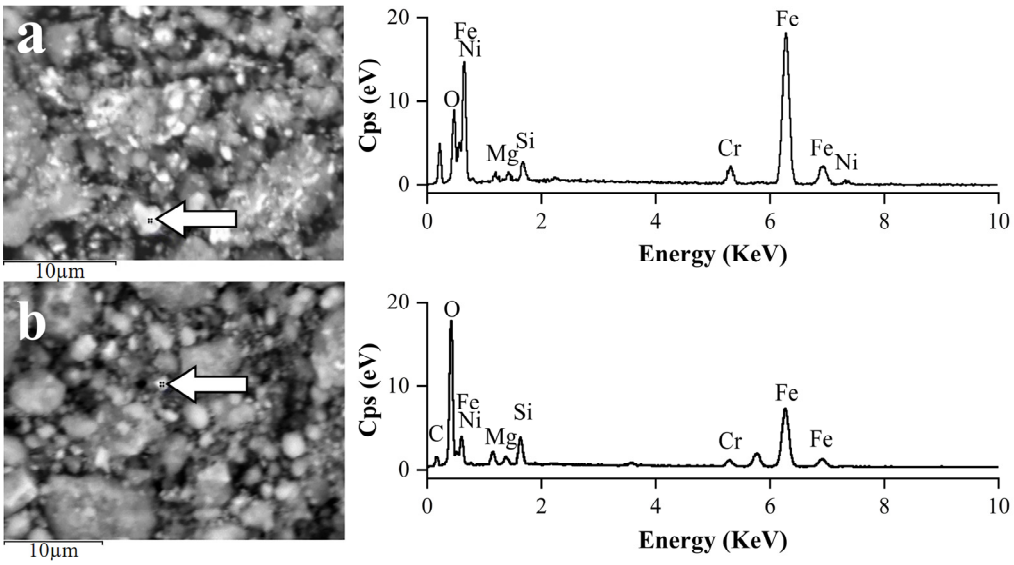

Figure 13. Backscatter spectra and energy spectra of concentrate (**a**) and tailings (**b**).

3.4. H_2-TPR Testing of the Reduction Reaction between Methane and Laterite Nickel Ore

In order to investigate the kinetics of methane reduction of laterite nickel ore, the hydrogen temperature programmed reduction technique (H_2-TPR) was used. During the experiment, the methane concentration was 100%, the heating rate was 10 °C/min, and the temperature range was between room temperature and 900 °C. The H_2-TPR spectrum was obtained as shown in Figure 14.

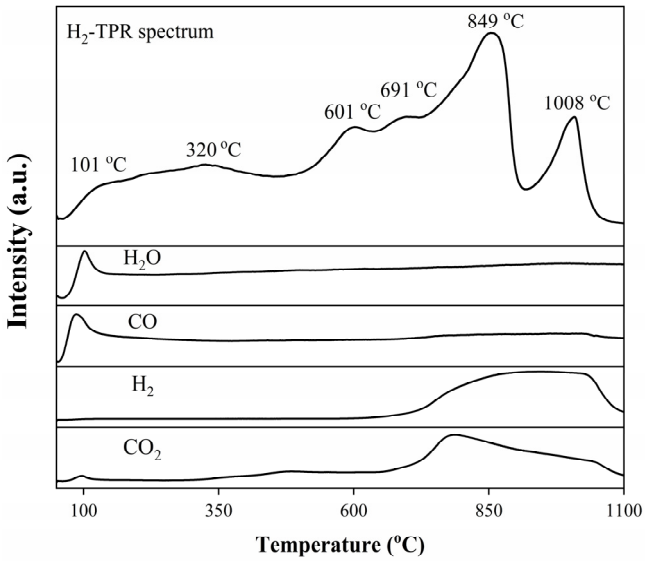

Figure 14. H_2-TPR spectrum of the laterite nickel ore and change trends of gases produced.

Figure 14 shows that there are five reduction peaks in the reaction between CH_4 and laterite nickel ore. There are significant fluctuations in the mass spectra of H_2O and CO within the temperature range of 57 °C–455.18 °C. At this stage, the reaction mainly involves the dehydroxylation of minerals such as goethite and serpentine, as well as the reduction of nickel iron oxide by CH_4 [25]. Within the temperature range of 455.18 °C–718.84 °C, the two reduction peaks of 601 °C and 691 °C indicate that CH_4 undergoes cracking and reduction reactions with iron and nickel oxides. However, there is almost no evidence to suggest the reduction effect of carbon black on carbon heat [26,27]. The reduction peak is strongest within the temperature range of 718.84 °C–911.13 °C, mainly due to

the accelerated cracking of CH_4, which generates a large number of hydrogen anion free radical reactions [28,29]. Within the temperature range of 911.13 °C–1077.18 °C, the decreasing trend of CO_2 concentration slows down. Mineral analysis shows that some calcium carbonate and magnesite are covered by magnesium silicate, and after high-temperature release, they decompose into carbon dioxide, calcium oxide, and magnesium oxide. The H_2-TPR spectral data echo the previous kinetic studies, further demonstrating the reaction conditions at different temperatures.

4. Conclusions

This article studied the medium-temperature reduction behavior of CH_4 and laterite-nickel ore, the mechanism of CH_4 reduction of laterite nickel ore and the reaction conditions under different reaction conditions. In addition, phase and microstructure analysis was conducted on various parts of the minerals during roasting and subsequent magnetic separation, and the tail gas during the roasting process was analyzed in isothermal reduction experiments combined with gas chromatography. This study found that:

(1) The optimal experimental conditions for this experiment are: a reduction temperature of 900 °C, a reduction time of 60 min, a CH_4 concentration of 50%, obtained nickel concentrate with a grade of 3.06% and a recovery rate of 52.09%.
(2) XRD and SEM characterization indicate that nickel in the concentrate mainly exists in the form of {Fe, Ni} alloys, while the unrecycled nickel in the tailings is mainly in the form of {Fe, Ni} alloys and occurs in $\{Fe,Mg\}_2SiO_4$. In addition, when the temperature is low, some nickel will be lost in the tailings filtrate, and the nickel recovery rate of this part is between 13 and 14%. The {Fe, Ni} alloys in the concentrate and tailings are relatively dispersed and do not agglomerate well. Moreover, due to the fine particle size of the {Fe,Ni} alloys in the tailings, they are not recovered into the concentrate during magnetic separation, resulting in a low grade and recovery rate of nickel.
(3) When CH_4 reduces laterite nickel ore at high temperatures, the H_2 produced synergistically reduces laterite nickel ore with CH_4, while the proportion of the carbon black-dominated carbothermal reduction reaction is very small. Thermodynamic studies have shown that CH_4 has a strong reducing ability. When the temperature exceeds 420 K, the NiO phase in the mineral is completely reduced, while iron oxides are reduced in the order of $Fe_2O_3 \rightarrow Fe_3O_4 \rightarrow FeO \rightarrow Fe$.
(4) The reason for the low nickel grade and recovery rate in the concentrate is, on the one hand, due to the incomplete reduction of NiO, as there is still a large amount of nickel present in the silicate in the tailings; on the other hand, it is due to the fine grain size of the partially reduced nickel iron alloy, which is lost in the tailings and filtrate. In order to improve the performance of magnetic separation, in future research, additives can be considered to improve the recovery rate of nickel.

Author Contributions: Methodology, Y.S.; validation, S.Q., formal analysis, X.L.; data curation, S.L.; investigation, J.Y.; project administration, S.Y. All authors have read and agreed to the published version of the manuscript.

Funding: This research was supported by the Fundamental Research Program of Shanxi Province of China (202203021212245), the Shanxi Provincial Science and Technology Achievement Transformation Guidance Special Program of China (202104021301052) and the Shanxi Provincial Patent Transformation Program of China (202306013).

Data Availability Statement: Data are contained within the article.

Conflicts of Interest: The authors declare no conflict of interest.

References

1. Zhang, Z.; Chen, X.; Li, Y.; Gao, A.; Wang, Y.; He, X.; Wang, Q. Multipurpose Utilization Trend of Nickel Mineral Resources under the Goal of Carbon Peaking and Carbon Neutrality. *Multipurp. Util. Miner. Resour.* **2022**, *43*, 31–39.
2. Wu, Q.; Cheng, C.; Ge, Z.; Ma, J. Thoughts on Ensuring the Supply Safety of Nickel Ore Resources. *China Min. Mag.* **2020**, *29*, 35–38.
3. Moskalyk, R.R.; Alfantazi, A.M. Nickel sulphide smelting and electrorefining practice: A review. *Miner. Process. Extr. Metall. Rev.* **2002**, *23*, 141–180. [CrossRef]
4. Ma, B.; Wu, H.; Gao, Z. Research development on treatment processes of laterite nickel ore. *Refract. Lime* **2022**, *47*, 35–40.
5. Zheng, Z. Current status and research of nickel ore resources pyrosmelting technology. *World Nonferrous Met.* **2023**, *13*, 4–6.
6. Zhao, D.; Ma, B.; Wang, C.; Chen, Y. Research progress of limonitic laterite hydrometallurgy. *J. Cent. South Univ. Sci. Technol.* **2023**, *54*, 401–414.
7. Ma, W.; Cheng, J. Development trend of low-grade nickel-laterite resources: The integrated model of "Resources+Energy+Materials". *China Nonferrous Metall.* **2019**, *48*, 75–78.
8. Abdul, F.; Pintowantoro, S.; Maulidani, A. Analysis the Effect of Charcoal Mass Variation to Ni Content, Sinter Strength and Yield on Sintering Process of Limonitic Laterite Nickel Ore. *Key Eng. Mater.* **2020**, *867*, 25–31. [CrossRef]
9. de Fátima da Silva, M.; de Sousa Oliveira, M.R.; dos Santos, I.D.; Radino-Rouse, P.; Mansur, M.B. Iron precipitation strategies from nickel laterite ore sulfuric acid leach liquor. *Miner. Process. Extr. Metall. Rev.* **2022**, *43*, 28–39. [CrossRef]
10. Faris, N.; Pownceby, M.I.; Bruckard, W.J.; Chen, M. The Direct Leaching of Nickel Sulfide Flotation Concentrates-A Historic and State-of-the-Art Review Part I: Piloted Processes and Commercial Operations. *Miner. Process. Extr. Metall. Rev.* **2022**, *44*, 407–435. [CrossRef]
11. Jiang, M.; Sun, T.; Liu, Z.; Kou, J.; Liu, N.; Zhang, S. Mechanism of sodium sulfate in promoting selective reduction of nickel laterite ore during reduction roasting process. *Int. J. Miner. Process.* **2013**, *123*, 32–38. [CrossRef]
12. Hu, C.; Jia, Y.; Liang, D.; Zhang, L.; Wang, X.; Li, S. Stduying on reductive roasting mechanism about nickel laterite. *China Nonferrous Metall.* **2012**, *41*, 72–75.
13. Sudagar, J.; Lian, J.; Sha, W. Electroless nickel, alloy, composite and nano coatings—A critical review. *J. Alloys Compd.* **2013**, *571*, 183–204. [CrossRef]
14. Mohanty, S.; Roy, S.K.; Sen, P.K. Thermodynamic considerations in reduction of nickeliferrous laterite by methane. *Metall. Mater. Trans. B* **2008**, *39*, 639–642. [CrossRef]
15. Su, K.; Wang, F.; Parianos, J.; Cui, Z.; Zhao, B.; Ma, X. Alternative Resources for Producing Nickel Matte-Laterite Ores and Polymetallic Nodules. *Miner. Process. Extr. Metall. Rev.* **2022**, *43*, 584–597. [CrossRef]
16. Liu, X.; Liu, S.; Yang, S. Reaction behavior of iron and nickel oxides in laterite nickel ore under action of methane. *Chin. J. Nonferrous Met.* **2022**, *32*, 1759–1771.
17. Li, B.; Ding, Z.; Wei, Y.; Zhou, S.; Wang, H. Reduction of nickel and iron from low-grade nickel laterite ore via a solid-state deoxidization method using methane. *Mater. Trans.* **2018**, *59*, 1180–1185. [CrossRef]
18. Wang, M.; Wang, Z.; Guo, Z. Water electrolysis enhanced by super gravity field for hydrogen production. *Int. J. Hydrogen Energy* **2010**, *35*, 3198–3205. [CrossRef]
19. Zhang, H.; Liu, H.; Ding, Z. Reduction roasting test of silicon-magnesium-type laterite-nickel ore under the action of methane. *J. Henan Univ. Sci. Technol. Nat. Sci. Ed.* **2018**, *39*, 6.
20. Pickles, C.; Anthony, W. Thermodynamic modelling of the reduction of a saprolitic laterite ore by methane. *Miner. Eng.* **2018**, *120*, 47–59. [CrossRef]
21. Kolmachikhina, O.; Polygalov, S.; Vakula, K. The study of physicochemical features of laterite ores of the buruktalsky deposit. *Solid State Phenom.* **2021**, *316*, 694–698. [CrossRef]
22. Al-Khirbash, S.A. Mineralogical characterization of low-grade nickel laterites from the North Oman Mountains: Using mineral liberation analyses-Scanning electron microscopy-based automated quantitative mineralogy. *Ore Geol. Rev.* **2020**, *120*, 103429. [CrossRef]
23. Tian, H.; Pan, J.; Zhu, D.; Yang, C.; Guo, Z.; Xue, Y. Improved beneficiation of nickel and iron from a low-grade saprolite laterite by addition of limonitic laterite ore and $CaCO_3$. *J. Mater. Res. Technol.* **2020**, *9*, 2578–2589. [CrossRef]
24. Zhang, Y.P.; Zhou, Y.H.; Li, Z.Y.; Li, W.G. Characteristics of laterite resource and analysis on its pyrometallurgy process. *Ferro-Alloys* **2007**, *6*, 18–21.
25. Quast, K.; Connor, J.N.; Skinner, W.; Robinson, D.J.; Addai-Mensah, J. Preconcentration strategies in the processing of nickel laterite ores Part 4: Preliminary dewatering studies. *Miner. Eng.* **2015**, *79*, 287–294. [CrossRef]
26. Wang, L.W.; Lü, X.M.; Liu, M.; You, Z.X.; Lü, X.W.; Bai, C.G. Preparation of ferronickel from nickel laterite via coal-based reduction followed by magnetic separation. *Int. J. Miner. Metall. Mater.* **2018**, *25*, 744–751. [CrossRef]
27. Yuan, S.; Zhou, W.-T.; Li, Y.-J.; Han, Y.-X. Efficient enrichment of nickel and iron in laterite nickel ore by deep reduction and magnetic separation. *Trans. Nonferrous Met. Soc. China* **2020**, *30*, 812–822. [CrossRef]

28. He, L.; Shen, Z. *Methane Conversion and Utilization*; Chemical Industry Press: Beijing, China, 2005.
29. Lu, J. Study on the Reduction of Sodium Sulfate to Laterite Nickel Ore Under Hydrogen and Methane Atmosphere. Master's Thesis, Taiyuan University of Technology, Taiyuan, China, 2013.